The Molecular Receptive Range of an Olfactory Receptor *in vivo* (*Drosophila melanogaster* Or22a)

Daniela Pelz,[1] Tina Roeske,[1] Zainulabeuddin Syed,[1]* Marien de Bruyne,[1]† C. Giovanni Galizia[1,2]

[1] Institut für Neurobiologie, Freie Universität Berlin, D-14195 Berlin, Germany

[2] Universität Konstanz, D-78457 Konstanz, Germany

Received 23 May 2006; accepted 19 July 2006

ABSTRACT: **Understanding how odors are coded within an olfactory system requires knowledge about its input. This is constituted by the molecular receptive ranges (MRR) of olfactory sensory neurons that converge in the glomeruli of the olfactory bulb (vertebrates) or the antennal lobe (AL, insects). Aiming at a comprehensive characterization of MRRs in *Drosophila melanogaster* we measured odor-evoked calcium responses in olfactory sensory neurons that express the olfactory receptor Or22a. We used an automated stimulus application system to screen [Ca^{2+}] responses to 104 odors both in the antenna (sensory transduction) and in the AL (neuronal transmission). At 10^{-2} (vol/vol) dilution, 39 odors elicited at least a half-maximal response. For these odorants we established dose-response relationships over their entire dynamic range. We tested 15 additional chemicals that are structurally related to the most efficient odors. *Ethyl hexanoate* and *methyl hexanoate* were the best stimuli, eliciting consistent responses at dilutions as low as 10^{-9}. Two substances led to calcium decrease, suggesting that Or22a might be constitutively active, and that these substances might act as inverse agonists, reminiscent of G-protein coupled receptors. There was no difference between the antennal and the AL MRR. Furthermore we show that Or22a has a broad yet selective MRR, and must be functionally described both as a specialist and a generalist. Both these descriptions are ecologically relevant. Given that adult *Drosophila* use approximately 43 ORs, a complete description of all MRRs appears now in reach.** © 2006 Wiley Periodicals, Inc. J Neurobiol 66: 1544–1563, 2006

Keywords: **olfaction; receptor neurons; molecular response profile; calcium imaging; *in vivo* recording**

INTRODUCTION

The identification of the olfactory receptor (OR) genes first in rats (Buck and Axel, 1991) and later in *Drosophila melanogaster* (Clyne et al., 1999; Gao and Chess, 1999; Vosshall et al., 1999) has initiated the molecular era of olfactory research. Now we know that olfactory sensory neurons (OSNs) express one or a few ORs (Vosshall et al., 2000; Dobritsa et al., 2003; Serizawa et al., 2003; Lewcock and Reed, 2004), that those OSNs that express the same OR(s) respond to the same odors (Hallem et al., 2004; Grosmaitre et al., 2006) and that they converge onto one or few glomeruli within the vertebrate olfactory bulb (OB) (Ressler et al., 1994; Vassar et al., 1994; Mom-

This article contains supplementary material available via the Internet at http://www.interscience.wiley.com/jpages/0022-3034/suppmat

*Present address: Department of Entomology, University of California, Davis, CA 95616.

†*Present address:* School of Biological Sciences, Monash University, Wellington Road, Clayton, Vic 3800, Australia.

Correspondence to: C.G. Galizia.

Contract grant sponsor: Volkswagenstiftung.

Published online 13 November 2006 in Wiley InterScience (www.interscience.wiley.com).
DOI 10.1002/neu.20333

baerts et al., 1996) or the insect antennal lobe (AL) (Couto et al., 2005; Fishilevich and Vosshall, 2005). Functionally, an OR is characterized by its olfactory ligands, which together constitute its molecular receptive range (MRR) (Mori and Shepherd, 1994; Araneda et al., 2000). The concept of MRR is not limited to the OR, but can also be applied for OSNs or any neuron population with homogeneous response properties. Although the binding properties of the OR itself determine most of the OSN's MRR (Hallem et al., 2004), other molecules, such as odor binding proteins, also contribute to the response profile (Xu et al., 2005). Interactions with additional receptors or signaling cascades further complicate the picture.

Ultimately, to understand olfactory coding it will be necessary to know the MRRs of each OSN. *Drosophila melanogaster* is an ideal model for achieving this goal (Stocker, 2001). Its olfactory system is complex yet numerically simple and in many respects similar to other olfactory systems (Stocker, 1994; Hildebrand and Shepherd, 1997). The adult *D. melanogaster* only expresses 43 OR genes (Vosshall et al., 2000; Couto et al., 2005; Fishilevich and Vosshall, 2005).

Here we present the first step toward determining the entire input range to the *Drosophila* olfactory system. We expressed the calcium sensitive protein *cameleon* under the control of the *Or22a* promotor. *Or22a* is expressed in one class of OSNs (ab3A) and its responses have already been characterized to some degree by electrophysiology (de Bruyne et al., 2001; Dobritsa et al., 2003; Stensmyr et al., 2003; Hallem et al., 2004; Hallem and Carlson, 2006), so our data can be validated. We measured the MRR *in vivo* by screening 104 odors across concentrations. We measured both at the level of sensory transduction in the antennal dendrites and cell bodies and at the level of sensory transmission at axon terminals in the AL. We show that Or22a has the same MRR on the antenna and in the AL. Or22a has a broad yet selective MRR being most sensitive to stimulation with *ethyl hexanoate* and *methyl hexanoate*, and less but still significantly sensitive to many other molecules. We describe molecular determinants common to activating odors of Or22a. We show that the broad response spectrum is ecologically relevant.

MATERIALS AND METHODS

Flies

Experimental animals were adult female *Drosophila melanogaster* at 1–3 weeks post-eclosion (age 15.5 ± 4.3 days, mean ± SD). Flies were F1 progeny from crosses between Cameleon 2.1 (w, UAS-> Cameleon 2.1, +) flies (Fiala et al., 2002) and Or22a (w; Cyo/Bl; P[Or22a->Gal4]/TM6B) flies (Vosshall et al., 2000). Flies were kept on a standard medium at a constant temperature of 25°C in an incubator and subjected to a 12h:12h light-dark cycle.

Confocal Pictures

Confocal pictures of flies expressing GFP under the Or22a promotor were acquired with a Leica DMRXE confocal microscope (Leica, Germany). Antennae were pulled from the fly's head and immediately placed in a solution of 60% glycerin dissolved in DMSO (Sigma, Germany), covered with a coverslip and scanned with a 20x air objective (NA = 0.7). Brains were prepared and dissected as for imaging (see below), and scanned with a 40x W NA = 0.8 objective. Excitation laser light was 488 nm. Z-stacks were taken at 1 μm axial resolution and projected onto a single plane employing WCIF ImageJ (http://www.uhnresearch.ca/facilities/wcif/).

In Vivo Preparation of Flies

Antennal Experiments. Flies were fixed in a 10 μL pipette tip such that the head just emerged. The heads' backs were fixed to the tube. Because Or22a positive cells are located on the antenna's dorso-medial side (Bhalerao et al., 2003; Dobritsa et al., 2003), we pulled one antenna backwards with a fine metal wire. A coverslip was placed onto the fly's head and a drop of H_2O was placed on top of the coverslip. The fly was now ready for imaging. Note that the preparation leaves the animal surgically intact.

Antennal Lobe Experiments. Flies were cooled for 30 min in a plastic vial on ice, fixed in a Perspex stage, and immobilized at their neck. The antennae were pulled forward with a fine wire. A polyethylene foil was sealed to the head with two-component silicon (KwikSil, WPI, FL, USA). A hole was cut into the foil, filled with saline (130 m*M* NaCl, 5 m*M* KCl, 2 m*M* $MgCl_2$, 2 m*M* $CaCl_2$, 36 m*M* saccharose, 5 m*M* hepes, pH 7.3) (Estes et al., 1996), and the head capsule was opened. Gland tissue, air sacks, and tracheae were removed, and the preparation was placed into the imaging setup. The AL preparation was superfused with fresh saline solution during the entire experiment.

Imaging

Antennal Experiments. The setup consisted of a microscope (Olympus BX50WI, Japan) equipped with a 20× W NA = 0.95 objective and a CCD/monochromator based imaging system (Till Photonics, Germany). Excitation wavelength was 435 nm. The primary dichroic mirror was 455 DCLP. The FRET-based [Ca^{2+}]-sensitive protein *Cameleon2.1* (Miyawaki et al., 1999) was imaged using a beam splitter (DualView, Optical Insights, USA), which split the

emitted light with a 505 dichroic and projected the two images on two halves of the same CCD chip, one through a BP 465-495 filter for ECFP (FRET donor), and the other through an LP 515 filter for EYFP (FRET acceptor). Images were taken at 3 Hz with an exposure time of 25 ms for each frame. Image size was 80 × 60 pixels, pixel size was 3.25 μm × 3.25 μm. To control for systematic differences between the two setups, some antennal recordings were done on the same setup as was in the AL experiments (see below), with image size 76 × 53 pixel, pixel size 3.2 μm × 3.2 μm, and an exposure time of 70 ms. There was no difference in the responses between the two setups.

Antennal lobe (AL) Experiments. AL experiments were done with a system that has been described earlier (Fiala et al., 2002). Briefly, excitation light came from a xenon lamp with a monochromator (Till Photonics, Germany), and imaging was done with two synchronized CCD cameras (TILL imago), one for each emission wavelength of *Cameleon2.1*. The microscope (Olympus BX51WI, Japan) was equipped with a 20× W NA = 0.95 dip objective, and an additional optical magnification of 1.25. Final resolution was (1.6 μm × 1.6 μm)/pixel, obtained by binning on chip to an image size of 153 × 106 pixel (corresponding to 244.8 μm × 169.6 μm). Excitation wavelength was 440 nm. The primary dichroic mirror was 470 DCLP. The emitted light was further split by a 520 dichroic and filtered with a BP 473-494 (ECFP, FRET donor) and a BP 530-565 (EYFP, FRET acceptor). Images were taken at a rate of 3 Hz, with an exposure time of 65–100 ms for each frame.

Odorant Preparation and Application

Odors were >99% pure or of the highest purity available (Sigma, Fluka, Aldrich; Germany). All chiral substances were racemic mixtures except for *ethyl (R)-(−)-3-hydroxy butanoate*; *ethyl (S)-(+)-3-hydroxy butanoate* and *(R)-(−)-carvone*; *(S)-(+)-carvone*. Pure odor substances were diluted in 5 mL mineral oil (Sigma–Aldrich, Germany) in 20 mL headspace vials (CleanPack, Germany) to their final concentration, ranging from 10^{-2} to 10^{-10} (vol/vol), and positioned in a computer-controlled autosampler (CombiPAL, CTC analytics, Switzerland). Headspace GC-FID analysis (Trace GC 2000, Thermo Electron Corporation, USA) of decadic concentration series showed that the logarithmic head space concentration decreased linearly with increasing odor dilutions.

A constant air stream (1 mL/s) coming from a synthetic air bottle (Messer-Griesheim, Germany) was guided through a glass-lined copper tube with an inner diameter of 1 mm. The tip was placed at a distance of 1 cm from the fly's antennae. During stimulation (2 s) the constant air stream was interrupted with a computer controlled solenoid valve and the autosampler injected 2 mL of headspace at a speed of 1 mL/s into the tube.

Each stimulus protocol consisted of blocks of 11 measurements, each with an interstimulus interval of 2 min. Each block started with three control measurements followed by eight odor presentations that either differed in their chemistry or in their concentration. The control measurements were: (1) a presentation of the diluent mineral oil, (2) room air, and (3) the reference odor. These blocks were repeated until responses to the reference odor decayed. Recordings from individual flies could show consistent responses for up to 160 min. The reference odor was used to monitor the fly's responsive state and to normalize responses. Normalization was necessary because absolute response values depended on many independent variables that affect fluorescence intensity, such as, cuticle pigmentation. Because the relative response value for each odor is affected by the variability in the reference stimulus, great care needs to be taken in the reference's choice. We sought for an odor that we could record at saturation, in order to avoid the linear range of the dose–response curve where small fluctuation greatly affect the response, and that would not be the best stimulus in order to reduce adaptation. On the basis of preliminary measurements the stimulus *ethyl propionate* at a concentration of 10^{-2} (vol/vol) was chosen as reference [compare with Fig. 2(b)].

Data Analysis

Data analysis was done with custom written IDL software (Research Systems, CO, USA). Measurements were chosen for further analysis if their flanking control blocks showed stable responses to the reference odor. First, the raw image data were corrected for lateral displacements to reduce movement artifacts. Images were spatially median filtered to reduce shot noise (size: 3 pixels). Then, the EYFP image was divided by the ECFP image and multiplied by 100 to yield Ratio (%). For antennal traces, averages of 11 × 11 pixel boxes were calculated as a function of time. For AL traces the boxes were 7 × 7 pixels [Fig. 1(C)]. Traces were shifted to baseline by subtracting the average of 6 time points before stimulus onset from the trace, and indicated as ΔRatio (%). For quantification of odor-evoked response magnitude, an average of three frames around the maximum of the response within 5 seconds after stimulus onset was taken. This time interval was chosen to include the maxima of slow responses that occurred for AL responses to low odor concentrations and for most antennal responses. Only one AL was evaluated in each animal, even though both antennae were stimulated, and both ALs responded.

To statistically analyze data across animals we normalized responses to the reference odor *ethyl propionate*. These values are indicated as "normalized response magnitude," or just *response*. Dose–response curves were established by first measuring the responses to a panel of 104 odors at a concentration of 10^{-2} (vol/vol). Subsequently all odors that elicited at least half-maximal responses were tested at a further tenfold dilution (10^{-3}). This procedure was repeated until no further response was measurable (for *ethyl hexanoate* at 10^{-10}).

Dose–response curves were created by averaging across animals for all tested concentrations of each odor. The Hill equation was fitted to the data (Meister and Bonhoeffer, 2001; Wachowiak and Cohen, 2001; Sachse and Galizia,

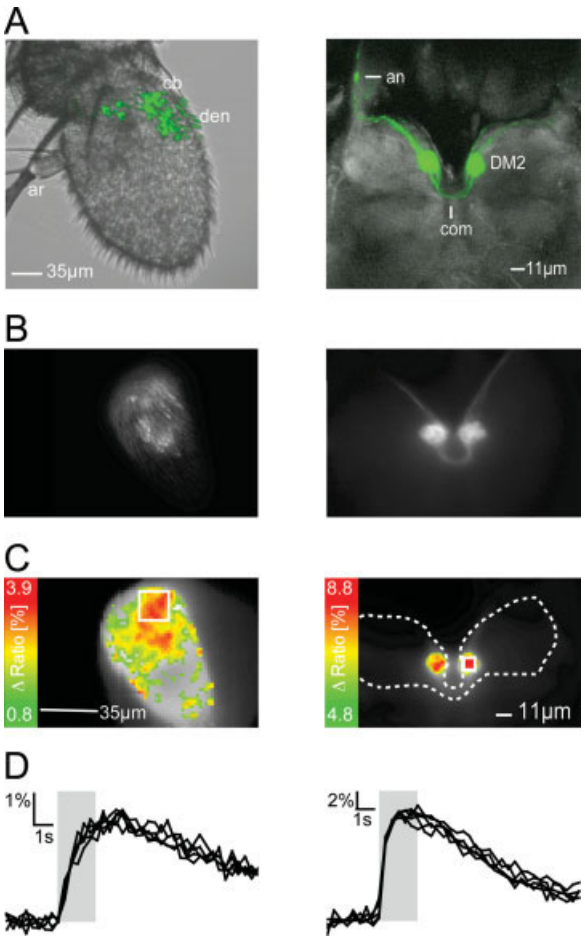

Figure 1 Calcium imaging on the antenna and in the AL. A: Confocal images of OSNs expressing CD8-GFP under control of the *Or22a* promotor. *Left:* antenna, ar, arista; cb, cell body; den, dendrites. *Right:* antennal lobe (AL), an, antennal nerve; DM2, glomerulus innervated by OSNs expressing *Or22a*; com, commissure formed by collateral OSN axons projecting to the contralateral AL. Orientation of the AL as in the preparation employed in this study. B: Images of the antenna (left) and the ALs (right) of cameleon expressed under control of the *Or22a* promotor. Orientation is as in panel A; images are taken with a CCD camera as for calcium imaging. C: False color-coded pictures of responses to *ethyl propionate* 10^{-2} measured on the antenna and in the AL, white squares indicate the area from which responses were calculated, orientation similar to panels A and B. The white dashed line indicates AL outline. D: Repeated responses to *ethyl propionate* 10^{-2} measured on the antenna (left) and the AL (right) over a time course of 100 min. Other odors were presented in between (not shown). Gray rectangle: stimulus. Y-axis shows ΔRatio (%).

2003), using a weighted nonlinear least squares algorithm (Motulsky and Christopoulos, 2004).

$$R(x) = R_{\max} \frac{x^n}{EC_{50}^n + x^n}$$

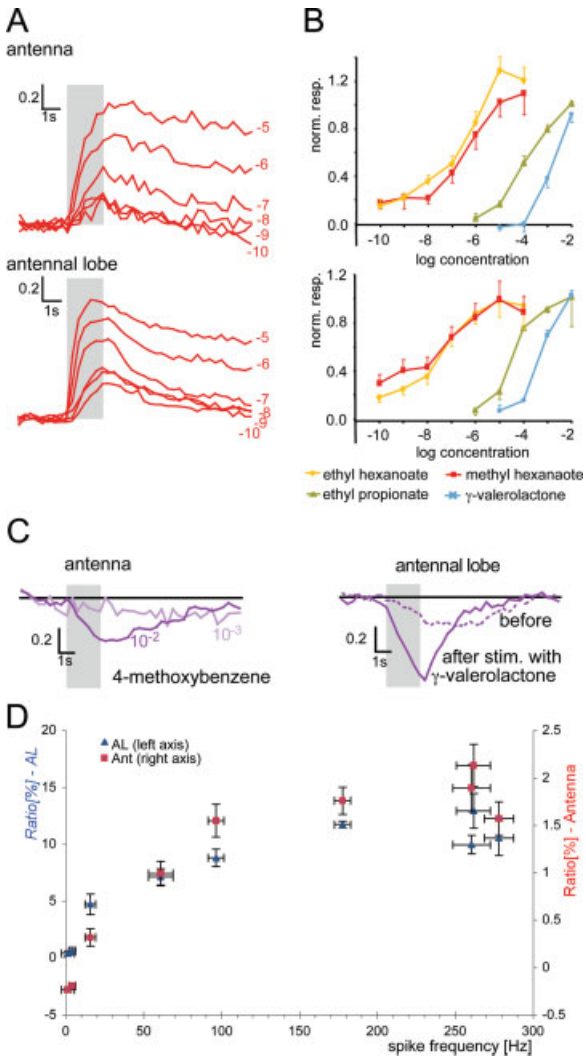

Figure 2 A: Responses to increasing concentrations of *methyl hexanoate* as measured on the antenna (upper panel, mean of 5 animals) and in the AL (lower panel, mean of 6 animals). Y-axis: normalized response strength. Numbers: log odor concentration (vol/vol). B: Exemplary dose–response curves (mean ± SEM) for *ethyl hexanoate* (orange), *methyl hexanoate* (red), *ethyl propionate* (green), and *γ-valerolactone* (blue). Color-odor labeling is maintained throughout all figures. **C:** Some odors lead to $[Ca^{2+}]$ decrease when presented at high concentrations. *Left:* antennal responses to *4-methoxybenzene* 10^{-2} ($n = 4$) and 10^{-3} ($n = 9$ animals). *Right:* AL responses to *4-methoxybenzene* 10^{-2} before and after presentation of *γ-valerolactone* 10^{-2} (mean of $n = 3$ animals). Y-axis: normalized response strength. E: Plot of spike frequency in ab3A neurons during the first 500 ms of an odor response (abscissa) against the calcium response on the antenna (right ordinate axis) and in the AL (left ordinate axis). See Methods for odor list. The relationship follows a monotonous saturating curve, with a section between approx. 15 and 200 Hz that is close to linear.

Experimentally determined values in the Hill equation are concentration x, the measured response for that concentration $R(x)$ (which entered the fitting algorithm as mean across animals with its variance as weight), and R_{max} for the overall maximal response to any odor. The estimated values are the Hill coefficient n, which represents a measure of the slope, and the *E*ffective *C*oncentration eliciting a half-maximal (i.e. 50%) response EC_{50}. Values for EC_{50} are given as decadic logarithms throughout this paper, for example $EC_{50}(AL) = -6.8$ indicates that a dilution of odor to $10^{-6.8}$ in mineral oil (vol/vol) as used in our apparatus (see earlier text) was determined to elicit half-maximal response in the AL.

Time traces among odorants were compared from estimated response traces at EC_{50} [e.g. in Fig. 6(C)]. The measured responses at the neighboring higher and lower concentrations were linearly interpolated for log-concentration at every time point separately.

Estimation of ppm

We converted vol/vol dilution to ppm in the stimulus, based on extensive published data about the relationship between liquid- and vapor-phase concentrations for 60 volatile organic compounds diluted in mineral oil (Cometto-Muniz et al., 2003). For substances that were not listed in that paper, we interpolated the values based on available vapor pressure information, and calculated 95% confidence limits for each odor (Table 1).

Nomenclature for Responsive Odors

In this paper, odors that evoked a $[Ca^{2+}]$ increase are called activating odors; odors that evoked a decrease in $[Ca^{2+}]$ are called inactivating odors; odors that did not evoke a change in fluorescence $[Ca^{2+}]$ are called non-activating odors. We avoided the more intuitive "ligand" or "agonist" terminology because the measured responses are cellular responses, which might be the result of several interactions. The binding of an odorant to the Or22a receptor (its "ligand" or "agonist" property) is likely the most important factor for the measured response, but not the only one: odor binding proteins, and/or other signaling cascades might alter the ligand spectrum and result in the "activating odor spectrum" measured here. Collectively, activating odors form the cell's MRR.

Electrophysiology

We calibrated our imaging methodology to well established electrophysiological methods. Odor responses were recorded extracellularly from Or22a-expressing neurons by inserting glass electrodes into individual ab3 sensilla on the *Drosophila* antenna as previously described (de Bruyne et al., 2001; Dobritsa et al., 2003). These sensilla contain two OSNs, one of which (ab3A) expresses Or22a. Neuronal excitation was measured as counts of spikes (action potentials) produced during the first 500 ms of the 2 s stimulation period. We and others have previously shown that spikes produced by the two neurons in such sensilla can be reliably separated based on amplitude and shape differences (de Bruyne et al., 2001; Stensmyr et al., 2003). The odors and concentrations used were *benzaldehyde* 10^{-2}, *1-butanol* 10^{-2}, *2-heptanone* 10^{-2}, *1-octen-3-ol* 10^{-2}, *ethyl 3-hydroxy hexanoate* 10^{-2}, *ethyl hexanoate* 10^{-2}, *heptanal* 10^{-2}, and *ethyl butanoate* 10^{-2} vol/vol for all dilutions. Each odor was further diluted 1:10 in the air stream. Odor delivery was as described in de Bruyne et al. (1999; 2001).

RESULTS

To characterize the molecular receptive range (MRR) of Or22a we raised flies expressing the ratiometric $[Ca^{2+}]$ sensor *Cameleon2.1* (Miyawaki et al., 1999; Fiala et al., 2002) under control of the *Or22a* promotor (Vosshall et al., 2000). In the antennal preparation, fluorescence was visible through the intact cuticle as one or two large areas in the dorsomedial position on the antenna both when we expressed GFP [Fig. 1(A), left] or *cameleon* [Fig. 1(B), left] under the control of *Or22a*. This area is in agreement with published data of ab3A OSNs where *Or22a* is expressed (de Bruyne et al., 2001; Bhalerao et al., 2003; Dobritsa et al., 2003). Presentation of an activating odor (i.e. an odor which elicited a response, see Materials and Methods) resulted in a clear signal in the fluorescent area [Fig. 1(C), left]. We did not observe any spatial response differences across the fluorescent area on the antenna, suggesting that OSNs expressing *Or22a* form a functionally homogenous population. Within a fly, repeated presentations of the same stimulus led to reproducible $[Ca^{2+}]$ responses for up to 160 min [Fig. 1(D), left, showing an example with 100 min]. Data on the antenna are based on 4244 odor presentations in 121 flies. Apart from the reference odor, no stimulus was given twice to the same animal. No animal received the entire odor panel (average number of stimuli per animal was 35.1 ± 18.7, a detailed list is given in Supplemental Table 3), and odor sequence differed from animal to animal. Absolute response magnitude to the reference odor *ethyl propionate* was 2.55 ± 0.79 Ratio(%), with no effect of age ($y = 2.14 + 0.03x$, with y being Ratio(%) response, and x being age in days; $R = 0.15$, $p = 0.196$).

In the AL preparation fluorescence could be seen in the antennal nerves, in one glomerulus in each AL and in the commissure between both ALs [Fig. 1(A,B), right]. This glomerulus has been identified as DM2 (Couto et al., 2005; Fishilevich and Vosshall,

Table 1 Odors Activating OSNs that Express Or22a

	Chemical Name	CAS#	EC_{50} ± SD AL	Hill Coeff. AL	EC_{50} ± SD Ant	Hill Coeff. Ant
Alcohol	1-Butanol	71-36-3	−3.10 ± 0.08	0.56	−2.40 ± 0.04	0.56
	3-Methyl-1-butanol	123-51-3	−2.92 ± 0.06	0.59	−2.47 ± 0.06	0.64
	1-Hexanol	111-27-3	−2.65 ± 0.10	0.87	−2.04 ± 0.08	0.73
	E2-hexen-1-ol[a]	928-95-0	−2.31 ± 0.06	0.54	*(0.50* ± 0.08)	
	Z3-hexen-1-ol[a]	928-96-1	−1.97 ± 0.07	0.53	*(0.49* ± 0.11)	
	4-Methylcyclohexanol[a]	25639-42-3	−2.15 ± 0.11	0.45	*(0.33* ± 0.10)	
	1-Heptanol[a]	111-70-6	−2.29 ± 0.10	0.55	*(0.26* ± 0.01)	
	1-Octen-3-ol	3391-86-4	−3.23 ± 0.09	0.69	−2.42 ± 0.07	0.57
	3-Octanol[a]	589-98-0	−2.80 ± 0.06	0.52	*(0.41* ± 0.11)	
Aldh.	Pentanal[a]	110-62-3	−2.91 ± 0.07	0.49	*(0.58* ± 0.03)	
	Hexanal[a]	66-25-1	−2.83 ± 0.05	0.40	*(0.56* ± 0.07)	
	Heptanal	**111-71-7**	**−4.81** ± 0.03	**0.41**	**−3.81** ± 0.03	**0.39**
Ester	Ethyl acetate[a]	141-78-6	−2.02 ± 0.03	0.24	*(0.48* ± 0.05)	
	Butyl acetate	**123-86-4**	**−4.33** ± 0.05	**0.58**	**−3.34** ± 0.03	**0.36**
	2-Methyl butyl acetate	**626-38-0**	**−4.89** ± 0.05	**0.55**	**−4.30** ± 0.03	**0.48**
	Pentyl acetate	**628-63-7**	**−4.53** ± 0.03	**0.52**	**−4.13** ± 0.02	**0.37**
	Iso-amyl acetate	**123-92-2**	**−4.16** ±0.03	**0.51**	**−4.01** ± 0.02	**0.39**
	Hexyl acetate	142-92-7	−2.61 ± 0.03	0.33	−2.74 ± 0.04	0.51
	E2-hexenyl acetate	2497-18-9	−3.37 ± 0.05	0.59	−3.22 ± 0.04	0.50
	Ethyl propionate	**105-37-3**	**−4.17** ± 0.04	**0.44**	**−3.12** ± 0.03	**0.42**
	Propyl propionate[b]	106-36-5	*(0.23* ± 0.13)			
	Ethyl butanoate	**105-54-4**	**−5.87** ± 0.02	**0.28**	**−4.35** ± 0.03	**0.44**
	Ethyl (*R*)-(−)-3-hydroxybutanoate	24951-95-5	−3.33 ± 0.07	0.79	−2.55 ± 0.05	0.60
	Ethyl (*S*)-(+)-3-hydroxybutanoate	56816-01-4	−2.84 ± 0.12	0.82	−2.11 ± 0.08	0.52
	Ethyl 2-methylbutanoate	**7452-79-1**	**−5.25** ± 0.02	**0.31**	**−4.33** ± 0.05	**0.39**
	Butyl butanoate	109-21-7	−2.85 ± 0.05	0.42	−2.86 ± 0.05	0.62
	Methyl pentanoate[b]	624-24-8	*(0.65* ± 0.06)			
	Ethyl pentanoate[b]	539-82-2	*(1.11* ± 0.07)			
	Methyl hexanoate	**106-70-7**	**−6.90** ± 0.03	**0.18**	**−6.00** ± 0.05	**0.32**
	Methyl 3-hydroxy hexanoate	21188-58-9	−3.62 ± 0.06	0.75		
	Ethyl hexanoate	**123-66-0**	**−6.83** ± 0.03	**0.25**	**−6.62** ± 0.03	**0.32**
	Ethyl 3-hydroxyhexanoate	2305-25-1	−3.27 ± 0.03	0.59	−2.43 ± 0.05	0.62
	Propyl hexanoate[b]	626-77-7	*(0.40* ± 0.04)			
	Methyl heptanoate[b]	106-73-0	*(0.30* ± 0.04)			
	Ethyl heptanoate[b]	106-30-9	*(0.30* ± 0.03)			
Ketone	2-Propanone[a]	67-64-1	−2.16 ± 0.07	0.58	*(0.44* ± 0.05)	
	2-Butanone[a]	78-93-3	−3.09 ± 0.07	0.74	*(0.60* ± 0.07)	
	3-Hydroxy-2-butanone[a]	513-86-0	−2.50 ± 0.11	0.55	*(0.44* ± 0.05)	
	2,3-Butanedione[a]	431-03-8	−2.91 ± 0.06	0.43	*(0.30* ± 0.11)	
	3-Penten-2-one	625-33-2	−3.50 ± 0.04	0.51	−3.02 ± 0.05	0.50
	2-Hexanone[a]	591-78-6	−3.03 ± 0.10	0.70	*(0.64* ± 0.08)	
	3-Hexanone	589-38-8	−3.12 ± 0.07	0.76	−2.40 ± 0.04	0.40
	Cyclohexanone[a]	108-94-1	−2.41 ± 0.12	0.74	*(0.40* ± 0.05)	
	2-Heptanon	110-43-0	−3.08 ± 0.04	0.49	−2.15 ± 0.03	0.38
O	β-butyrolactone	3068-88-0	−2.56 ± 0.05	0.56	−2.16 ± 0.06	0.55
	γ-valerolactone	108-29-2	−2.87 ± 0.03	0.77	−2.38 ± 0.15	0.86

CAS #: chemical abstract service number; EC_{50} ± SD AL/ant: logarithm of estimated EC_{50}, see text, for antennal lobe (AL) and antenna, respectively. Also see a complete list with all measured parameters in Supplemental Table 1.

[a] Antennal responses did not reach a half-maximal response at 10^{-2} (vol/vol), values given for the antenna are mean normalized response ± SEM at 10^{-2} (vol/vol) and put into brackets for clarity.

[b] Tested at a concentration of 10^{-6} (vol/vol) within the AL, values given are mean normalized response ± SEM and put into brackets for clarity. The 10 strongest stimuli are given in bold. Aldh.: aldehyde, O: O-ring.

2005) in the AL atlas (Stocker et al., 1990; Laissue et al., 1999). Presentation of an activating odor led to an odor response in both glomeruli [Fig. 1(C), right]. In *Drosophila*, OSN axons innervate olfactory glomeruli in both antennal lobes. We always stimulated both antennae, and therefore recorded the compound response of cells from the ipsilateral and from the contralateral antenna. No attempt was made to quantify the relative contribution of each antenna. The time course of a $[Ca^{2+}]$ response to repeated presentations of the same stimulus was highly reproducible [Fig. 1(D), right]. A total of 100 flies were measured for the AL, with 2982 odor presentations. Apart from the reference odor, no stimulus was given twice to the same animal. No animal received the entire odor panel (average number of stimuli per animal was 29.8 ± 12.7, a detailed list is given in Supplemental Table 3), and odor sequence differed from animal to animal. Absolute response magnitude to the reference odor *ethyl propionate* was 9.57 ± 2.68 Ratio (%), with responses increasing slightly with age ($y = 5.48 + 0.27x$, with y being Ratio (%) response, and x being age in days; $R = 0.41, p < 0.001$).

Responses increased with increasing odor concentration both on the antenna and in the AL [Fig. 2(A)]. Dose–response curves showed a typical sigmoid shape [Fig. 2(B)] with similar saturation levels for different odorants. The more potent odorants elicited responses from Or22a neurons at lower doses, resulting in lateral displacement of these dose–response curves.

On the antenna, a few odors gave negative responses when tested at high concentrations, i.e. $[Ca^{2+}]$ levels decreased after stimulation. These were: *4-methoxybenzene*, *benzaldehyde*, *4-methoxybenzaldehyde*, and *(1R)-(−)-fenchone* (Supplemental Table 2). We did not observe any negative responses in the AL (see Supplemental Table 2). For example, on the antenna *4-methoxybenzene* did not evoke a response at a concentration of 10^{-3} but led to a decrease in calcium at the higher concentration of 10^{-2} [Fig. 2(C), left], while in the AL *4-methoxybenzene* (10^{-2}) did not elicit any significant $[Ca^{2+}]$ change [Fig. 2(C), right, dotted line]. This difference might be due to differences in the resting calcium level, which could be within the dynamic range of dendrites or somata on the antenna. The spontaneous AP frequency in Or22a-OSNs was about 4 Hz (see below), and the reduction in intracellular calcium in the axonal terminals when this frequency drops is likely to be below the detection threshold of *Cameleon2.1*. If negative responses could not be observed in the AL because of low background activity, then an elevation of the resting calcium level by a preceding stimulus should allow to unmask *4-methoxybenzene* as an inactivating odor also in the AL. Indeed, in the AL a decrease in $[Ca^{2+}]$ was visible when *4-methoxybenzene* (10^{-2}) was presented after presentation of an odor with a long-lasting response, e.g. *γ-valerolactone* (10^{-2}) [Fig. 2(C), right, continuous line]. We observed the same effect for *benzaldehyde* 10^{-2} (data not shown). These observations do not preclude that interactions within the AL might cause or contribute to this effect.

OSNs that express *Or22a* have their dendrites in basiconic sensilla that can be specifically targeted by extracellular electrophysiological recordings, and are called ab3A (ab for antennal basiconic) (Dobritsa et al., 2003). We used electrophysiological recordings to calibrate our $[Ca^{2+}]$ signals [Fig. 2(D)]. Spontaneous activity in ab3A was 4 ± 2.4 Hz (mean ± SD), corresponding to published values for ab3A (de Bruyne et al., 2001; Dobritsa et al., 2003; Hallem et al., 2004). Response frequency during the first 500 ms of the response saturated below 300 Hz [Fig. 2(D)]. The relationship between $[Ca^{2+}]$ responses and spiking frequency in ab3A followed a saturating exponential trajectory, with an approximately linear segment over the range between 15 Hz and close to 200 Hz. The range between 4 Hz and 15 Hz was very steep. Optical responses were weaker on the antenna when compared with the AL, but the range of good correspondence between spike counts and optical responses was comparable [note the two separate ordinates in Fig. 2(D)]. In the *Drosophila* neuromuscular synapse, using *cameleon3.3*, the minimum spiking frequency for a presynaptic calcium signal was found to be in the range of 5–10 Hz (Reiff et al., 2005). However, the response range of *cameleon3.3* is shifted to the right with respect to *cameleon2.1* used here (Miyawaki et al., 1999), and consequently *cameleon2.1* is able to detect even lower $[Ca^{2+}]$, corresponding to fewer spikes.

The MRR of OR22a

We characterized the MRR of Or22a in two steps. In the first step we took a "shot gun" approach by screening the responses to substances from 9 different chemical classes (acids, alcohols, aldehydes, aromatics, ketones, N-rings, esters, O-rings, terpenes). The molecules ranged from C_3 to C_{20}. We tested saturated and unsaturated straight chains, branched chains, cyclics, and other chemical features (see Tables 1 and 2, and Supplemental Tables 1 and 2). In a second step we systematically altered the chemical

structure of the most efficient stimulus in order to define the "peak" of the MRR in more detail (Araneda et al., 2000; Spehr et al., 2003).

In the "shot gun" approach we started with a high concentration (10^{-2} (vol/vol)) in order to identify even weak ligands. To adjust for differences between individuals, responses were calculated as relative signals by setting the response to *ethyl propionate* to 100%. Out of 104 tested substances 39 elicited at least a half-maximal response in the AL at 10^{-2}. In the AL the maximal response was elicited by *ethyl 2-methyl butanoate* at a concentration of 10^{-2} (1.31 ± 0.33; mean ± SEM, $n = 3$). Note that the maximal response was not elicited by the stimulus with the lowest EC_{50}. We measured the dose–response curves for each of these 39 activating odors [Fig. 2(B)]. Ten of the 39 activating odors reached saturation (defined as a response increase of less than 10% for the next decadic concentration step). We fitted the Hill equation and estimated Hill coefficients and EC_{50} values. The Hill coefficient values were normally distributed (Kolmogorov-Smirnov normality test passed with $p = 0.115$). They were all below 1 (see Table 1) (0.53 ± 0.17; mean ± SD). These low Hill coefficient values correspond to a shallow dose–response curve that spanned about 3–4 log units [Fig. 2(B)]. Using $[Ca^{2+}]$ measurements cannot create a broader response range, but if anything, could create a steeper curve, so that our finding of 3–4 log units dynamic range is a conservative estimate. This is because the response of a calcium indicator is the convolution of the cellular calcium response with the fluorescence response of the indicator. In the case of *cameleon2.1* used here, the indicator follows a biphasic trajectory, with a lower response shank ($K_D = 100$ nM, Hill coeff. $n = 1.8$) and a high, more shallow response shank ($K_D = 4.3$ μM, Hill coeff. $n = 0.6$), covering a $[Ca^{2+}]$ range from 30 n*M* to 100 μM (Miyawaki et al., 1999). Shallow dose–response curves were also reported from identified OSNs in the mouse olfactory epithelium (Grosmaitre et al., 2006), and from glomerular measurements in mice (Wachowiak and Cohen, 2001) and honeybees (Sachse and Galizia, 2003). However, individual dissociated OSNs have much steeper dose–response curves, in the range of 1–2 log-units (Reisert and Matthews, 2001; Bozza et al., 2002; Takeuchi and Kurahashi, 2005). When measuring a population response, as in our case, individual OSNs with shifted sensitivity might lead to an increased dynamic range for the averaged population. However, the correspondence of our calcium response range with the electrophysiological range of individual OSNs (Fig. 2(D) would argue that in *Drosophila* individual OSNs cover the entire dynamic range observed here, as shown for single sensilla recordings (Dobritsa et al., 2003). EC_{50} values differed widely for the 39 activating odors measured in the AL, as shown in Figure 3(A).

On the antenna the maximal response was elicited by *2-methyl butyl acetate* at a concentration of 10^{-2} (mean ± SEM: 1.39 ± 0.05, $n = 12$). Generally, dose–response curves for the antenna were shifted to higher concentrations in comparison with the AL dose–response curves, leading to systematically higher EC_{50} values [Fig. 3(B)]. As a consequence, 14 odors did not reach a half-maximal response on the antenna at 10^{-2}, and only the remaining 25 odors had sufficient data points to fit the Hill equation. For these odors, a comparison between data from the antenna and the AL gave a strong linear correlation [$EC_{50(AL)} = 1.02 \times EC_{50\ (ANT)} - 0.58$; $R^2 = 0.91$; Fig. 3(B)], where the offset of −0.58 corresponds to the right-shift of antennal dose–response curves. There was some scatter at the lower response end, which we did not investigate any further. Hill coefficients from the antenna were also normally distributed (Kolmogorov-Smirnov normality test passed with $p > 0.2$). There was no significant difference between the antennal and the glomerular Hill coefficients (paired *t*-test, $t = 0.786$, df = 48, $p = 0.436$). We conclude that antenna and AL have qualitatively the same MMRs.

Or22a Odotopes

The parts of an odor molecule responsible for the interaction of this odor with a particular receptor have been termed odotopes (Mori and Shepherd, 1994; Malnic et al., 1999). We therefore analyzed whether the response spectrum of Or22a was predictable by a particular molecular feature. The response spectrum was broad (39 out of 104 odors tested, Fig. 3), but by no means arbitrary. First, there were clear exclusion criteria: none of the aromates, terpenes or acids tested elicited a response (Table 2 and Supplemental Table 2), with the exception of *propionic acid* that elicited a small response at the highest concentration 10^{-2}. We tested substances with molecular weight between MW = 58 U and MW = 310 U (Supplemental Table 2), but responses were only seen in the range 58–160 U, indicating that there is an upper limit for molecule size. There was no other relationship of molecular size with response strength, in the sense that within the permissive range substances with equal MW could elicit vastly different responses. We tested molecules in the range C_3–C_{20}. Most activating odors had a carbon backbone in the range of C_6–C_8, but some activating odors reached down to C_4 (Supplemental Table 1). We tested 2 enantiomeric substances separately, and found that in one case chirality influences the response: *ethyl-R-*

Table 2 Odors that did not Elicit Responses in OSNs that Express Or22a

	Chemical Name	CAS#
Acid	Propanoic acid[a]	79-09-4
	2-Methyl propanoic acid	79-31-2
	Butanoic acid	107-92-6
	3-Methylbutanoic acid	503-74-2
	Pentanoic acid	109-52-4
	Heptanoic acid	111-14-8
	Nonanoic acid	112-05-0
Alcohol	2,3-Butanediol	513-85-9
	Cyclohexanol	108-93-0
	Octanol	111-87-5
	Decanol	112-30-1
Aldehyde	Propanal	123-38-6
	E2-hexenal	6728-26-3
	Octanal	124-13-0
	Decanal	112-31-2
Aromatic	Phenylacetaldehyde	122-78-1
	Salicyl aldehyde	90-02-8
	2-Hydroxy-anisole	90-05-1
	4-Propenyl anisole	104-46-1
	Benzaldehyde[b]	100-52-7
	4-Methoxybenzaldehyde	123-11-5
	4-Isopropylbenzaldehyde	122-03-2
	4-Methoxybenzene[b]	100-66-3
	4-Allyl-1,2-Dimethoxybenzene	93-15-2
	2,4,5-trimethoxy-1-propenylbenzene (trans)	2883-98-9
	Benzyl cyanide	140-29-4
	2-Phenylethanol	60-12-8
	Phenylethanone	98-86-2
	Eugenol	97-53-0
	Iso-eugenol	97-54-1
	4-Methylphenol	106-44-5
	4-Ethylphenol	123-07-9
	2-Propylphenol	644-35-9
	3-Phenyl-2E-propenal	14371-10-9
	Methylsalicylate	119-36-8
	Octyl acetate	112-14-1
	Decyl acetate	112-17-4
Ester	Methyl propionate[c]	554-12-1
	Methyl butanoate[c]	623-42-7
	Propyl butanoate[c]	105-66-8
	Hexyl butanoate	2639-63-6
	Propyl pentanoate[c]	141-06-0
	Butyl hexanoate[c]	626-82-4
	Nonanone	821-55-6K
	Indole	120-72-9N
O-ring	Furfural	98-01-1
	Acetyl furan	1192-62-7
	γ-pentyl-γ-butyrolactone	104-61-0
Terpene	(*R*)-(−)-carvone	6485-40-1
	(*S*)-(+)-carvone	2244-16-8
	1,8-Cineole	470-82-6
	β-citronellol	106-22-9
	Citral	5392-40-5
	(*S*)-(−)-Citronellal	106-23-0
	(1*R*)-(−)-Fenchone	7787-20-4
	Geraniol	106-24-1
	Geranyl acetate	105-87-3
	(*R*)-(+)-limonene	5989-27-5
	Linalool	78-70-6
	(−)-Menthone	14073-97-3
	(1*R*)-(−)-myrtenal	564-94-3
	(+)-α-pinene	7785-70-8
	(*R*)-(+)-pulegon	89-82-7
	α-terpineole	10482-56-1
	(−)-α-thujone	546-80-5
	α-bisabolol	515-69-5
	β-caryophyllene	87-44-5
	E,E-farnesol	106-28-5
Other	Heptane	142-82-5
	Octane	111-65-9
	Nonane	111-84-2
	Z11-Hexdecenyl acetate	34010-21-4
	Z11-Octadecenyl acetate	1775-43-5

CAS #: chemical abstract service number; k: ketone; N: N-ring.
[a] Odor elicited a small response at 10^{-2} (vol/vol).
[b] Inactivating odor. Also see Supplemental Table 2 for measured parameters.
[c] Odor was only tested at a concentration of 10^{-6} (vol/vol).

(−)-3hydroxybutanoate elicited a stronger response than *ethyl-S-(+)-3hydroxybutanoate* ($EC_{50} = -3.3$ vs. $EC_{50} = -2.8$, Fig. 3, Table 1). While *(S)-(+)-carvone* elicited a stronger response than *(R)-(−)-carvone* (0.27 vs. 0.14 relative *response* at 10^{-2}, Table 2 and Supplemental Table 2), both enantiomers did not reach responses above the control levels of air or solvent stimulation, and are therefore not considered significant stimuli.

The two best stimuli were *ethyl hexanoate* ($EC_{50\ (AL)} = -6.8$; $EC_{50\ (ANT)} = -6.6$) and *methyl hexanoate* ($EC_{50\ (AL)} = -6.9$; $EC_{50\ (ANT)} = -6.0$), two substances that smell like pineapple to humans. These two substances had already been identified from fruit in GC linked electrophysiological recordings on the *Drosophila* antenna (Stensmyr et al., 2003). The next best odor *ethyl butanoate* had an EC_{50} more than 10 times lower (see Fig. 3 and Table 1). Esters from C_5 to C_8 made up 9 out of the 10 best substances. The aldehyde *heptanal* was the only non-ester among the first decade. Other activating odors included alcohols, ketones and O-rings [Fig. 3(A), Table 1, Supplemental Fig. 1], and several esters did not elicit a response at all (*octyl acetate, decyl acetate, hexyl butanoate*), indicating that the MRR is not related to the func-

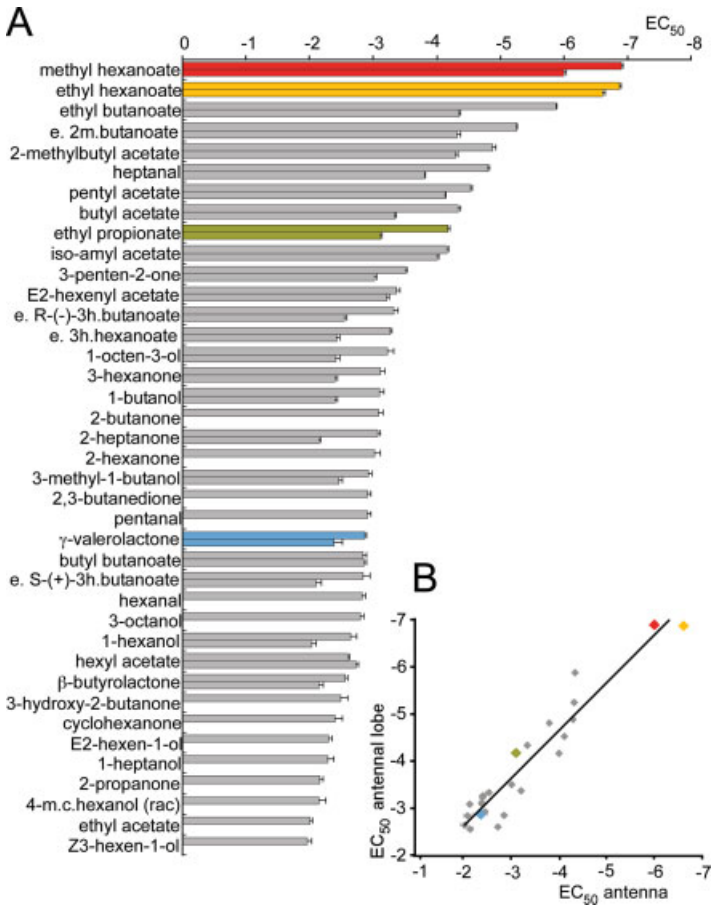

Figure 3 Molecular receptive range of Or22a. A: Odor sensitivity (EC_{50} values ± SD) for 39 substances in the AL (upper bars) and 25 substances on the antenna (lower bars). Four odors are color coded [see Figure 2(B)]. B: Correlation between EC_{50} values on the antenna and in the AL, showing a strong linear relationship (see text).

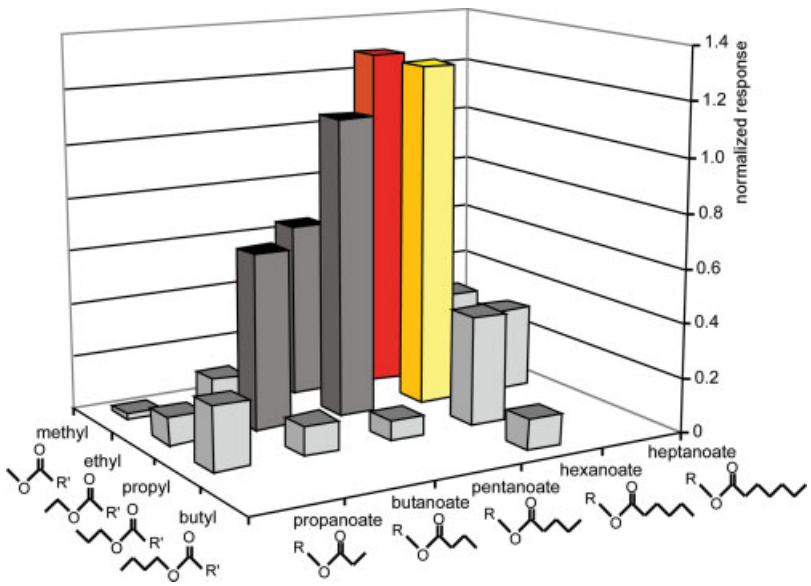

Figure 4 *Ethyl hexanoate* and *methyl hexanoate* are the most efficient stimuli for Or22a. The graph shows the ''molecular landscape'' surrounding the best odors. Normalized responses to a concentration of 10^{-6} ($n = 8$ animals, Z-axis; SD see Table 1) are plotted for straight chain esters with carboxylic acid moieties ranging from C_3 – *propanoate* to C_7 – *heptanoate* (X-axis) and alcohol moieties ranging from C_I – *methyl* to C_{IV} – *butyl* (Y-axis).

tional group alone. The ketone eliciting the strongest response was *3-penten-2-on* with $EC_{50} = -3.5$, the strongest alcohol was *1-octen-3-ol* with $EC_{50} = -3.2$, the second aldehyde after heptanal was pentanal with $EC_{50} = -2.9$ [Fig. 3(A), Table 1].

The length of both the alcohol and the carboxylic acid moiety forming the ester influenced the response: the esters *ethyl hexanaote* and *hexyl acetate* have the same molecular formula ($C_8H_{16}O_2$) but the molecules differ from each other in that *ethyl hexanoate* consists of a C_2 alcohol and a C_6 carboxylic acid whereas *hexyl acetate* consists of a C_6 alcohol and a C_2 carboxylic acid. *Ethyl hexanoate* had a very low EC_{50} ($EC_{50} = -6.8$) whereas *hexyl acetate* had an EC_{50} that was approx. 16,000 times higher ($EC_{50} = -2.6$). We systematically investigated the role of each ester sidegroup. For this experiment we used the concentration of 10^{-6}. At this concentration both *ethyl hexanoate* and *methyl hexanoate* elicit very strong responses [Fig. 2(B)]. We varied the alcohol moiety (ranging from C_I – *methyl* to C_{IV} – *butyl*, shortened here with C and Latin subscript number) and the carboxylic acid moiety (ranging from C_3 – *propionate* to C_7 – *heptanoate*, shortened here with C and Arabic subscript number). *Ethyl hexanoate* (C_{II}-C_6) and *methyl hexanoate* (C_I-C_6) were confirmed as the best stimuli [see Fig. 4]. The preferred carboxylic acid moiety was C_6 – *hexanoate*, the preferred alcohol moiety was a C_{II} – *ethyl*. The preference for an *ethyl* over a *methyl* group became apparent when the carboxylic acid moiety was shorter than C_6 – *hexanoate* (e.g. *ethyl pentanoate* elicited a stronger response than *methyl pentanoate*).

As observed in the large screen (''shot gun'' approach, above), there was a size limit for esters, indicating that repulsive forces may become important at longer molecular lengths or that the interaction site imposes steric constraints: esters C_9 and larger (*propyl hexanoate*, *butyl hexanoate*, *ethyl heptanoate*) elicited rather small responses, just above the noise level. Additionally, esters below C_6 (*methyl propionate, ethyl propionate, methyl butanoate*) did not elicit a response. A size limit was not only apparent for the entire molecule, but also for each moiety individually. For the alcohol moiety the limit was C_{II} whereas *methyl hexanoate* and *ethyl hexanoate* both elicited a large response (C_I: 1.28 ± 0.05, C_{II}: 1.27 ± 0.03, mean ± SEM), *propyl hexanaote* only elicited a very small response (C_{III}: 0.40 ± 0.04) and *butyl hexanote* did not elicit a response at all (C_{IV}: 0.11 ± 0.02). Additionally, none of the propyl esters elicited a large response (C_V: *propyl pentanoate*: 0.07 ± 0.03, *propyl butanoate*: 0.11 ± 0.03, *propyl propionate*: 0.23 ± 0.05). Also for the carboxylic acid moiety, increasing the chain length had a stronger effect than decreasing it. On the two sides of the optimal C_6, *methyl heptanoate* (0.30 ± 0.04) and *ethyl heptanoate* (0.30 ± 0.03, both C_7) elicited much smaller responses than *methyl pentanoate* (0.65 ± 0.06) and *ethyl pentanoate* (1.11 ± 0.06, both C_5). From these observations we conclude that, compared with the best stimulus, molecules that are shorter interact better with the receptor than those that are longer.

Relationship of vol/vol Dilution with ppm Estimation

We used vol/vol dilution for our concentration series. Ecologically, that would correspond to odor sources (say, rotting fruit) with different concentrations of a substance in the liquid substrate. Mechanistically, however, odor-responses elicited at the OSNs are based on stochiometric events that depend on the number of interacting molecules, and therefore on the number of odor molecules in the air, rather than on their concentration in the solvent. Because vapor pressure differs for different substances, the relationship of liquid dilution and ppm concentration in the air is not linear. Plotting EC_{50} values against (*ppm odor molecules/air volume*) rather than plotting them against (*odor volume/liquid solvent volume*) could potentially alter the response spectrum. There is no universal formula to convert vol/vol into ppm (Cometto-Muniz et al., 2003). Therefore, we estimated the ppm at EC_{50} for 23 odors for which published data could be adapted (see Materials and Methods and Supplemental Table 1). We found a highly significant linear relationship between EC_{50} values in vapor ppm when plotted against EC_{50} values in vol/vol dilution (see Fig. 5), with a slope close to 1 ($EC_{50}(\text{ppm}) = 1.06 \times EC_{50}$ (vol/vol) + 5.06, $R^2 = 0.72$). The scatter is minor, and does not qualitatively change the spectrum shown in Figure 3. Even in ppm-units, the best odors were *ethyl hexanoate* and *methyl hexanoate*, and the sequence of next-best stimuli was effectively unchanged (Supplemental Table 1). This is a consequence of the fact that the molecules contained in the response spectrum span a limited range in volatility.

Time Courses of $[Ca^{2+}]$ Responses Differ between Odors

As reported above, the response spectrum was very broad (39 activating odors out of 104 tested odors). This analysis is based on the maximal $[Ca^{2+}]$ increase, irrespective of the time-course of the response. However, odor-evoked response show clear temporal dynamics already at the level of OSNs (de

Bruyne et al., 2001), and accordingly we found a range of different time courses in odor-evoked [Ca^{2+}] responses, differing in response onset time, the slope of the rising flank, and the slope of the falling flank. Due to the intrinsic slowness of calcium signals with the sensor *cameleon*, sharp signal decreases could not be determined. However, temporal complexities resulting in delayed calcium increases should be visible with the techniques used here. We did not find any temporally complex response properties. In particular, there were no off responses (i.e. calcium increases at the end of the stimulus), nor any double peak responses.

We quantified the time point of response onset, rise time (defined as time interval on the rising flank between 10% and 90% of maximum), time point of peak response, fall time (defined as time interval on the falling flank between 90% and 66% of maximum) and overall response duration (defined as time interval between 10% of the maximum before and 66% after response peak, see Fig. 6(A)). The concentration dependent time courses of [Ca^{2+}] responses were reproducible across animals for each odor. However, for a given odor the time-course shape changed with changing odor concentration [Fig. 6(B)]. Response duration and fall time both increased with increasing odor concentration for antennal as well as for AL responses. In the AL rise time decreased with increasing odor concentration leading to an earlier response peak. On the antenna, however, rise time increased with increasing odor concentration and the response peak occurred later. This effect is quantified in Figure 6(B) for *methyl hexanoate*; compare with the response traces in Figure 2(A).

In order to remove the concentration effect when comparing temporal parameters across odors we calculated response traces with half-maximal responses, i.e. as if stimulus concentrations were selected at EC_{50}. These traces were interpolated from the time traces at the concentration below and above EC_{50}. Three examples are shown in Figure 6(C) for antenna and AL, respectively, and repeated for direct comparison. *Ethyl propionate* had a short rise time and fall time, *methyl hexanoate* also had a short rise time but a longer fall time, and *γ-valerolactone* had a late response onset and elongated rise time and fall time. These three time-courses were individual cases in a continuum of different shapes that could not be classified into clear groups. We therefore wondered whether there was a numerical relationship between the odor's efficacy (EC_{50}) and any of the response shape parameters. However, there was no such relationship in the AL [Fig. 6(D)] and not in the antenna (Supplemental Table 1). We conclude that temporal response properties and stimulus efficacy are independent parameters. Since the calcium signals that we measure are likely to be a combination of several calcium sources, a mechanistic interpretation of this temporal variability is not possible at this stage.

Across odors, response characteristics were correlated between the AL and the antenna. However, there was a systematic effect of antenna vs. AL, in that antennal responses had a delayed response onset (AL = 2.75 s, antenna = 2.90 s, $p \leq 0.001$ Wilcoxon signed rank test), a longer rise time (AL = 1.04 s, antenna = 1.41 s, $p \leq 0.001$), a delayed response peak (AL = 3.79 s, antenna = 4.33 s, $p \leq 0.001$), and longer fall times (AL = 1.32, antenna = 1.82, $p \leq 0.001$). These differences are likely due to the different calcium sources in the antennal dendrites and cell bodies as opposed to the axonal endings in the AL.

Chemical Moieties Systematically Influence Temporal Response Parameters

Though there was no correlation between an odor's response time course and its EC_{50} value, there were systematic effects related to the odor's chemistry. An additional hydroxyl group at the 3rd carbon atom of the carboxyl acid moiety of the esters *ethyl hexanoate*, *methyl hexanoate* and *ethyl butanoate* led to a consistently longer rise time as compared to the esters without that group, both on the antenna and in the AL [Fig. 7(B,C), antennal data not shown]. The addi-

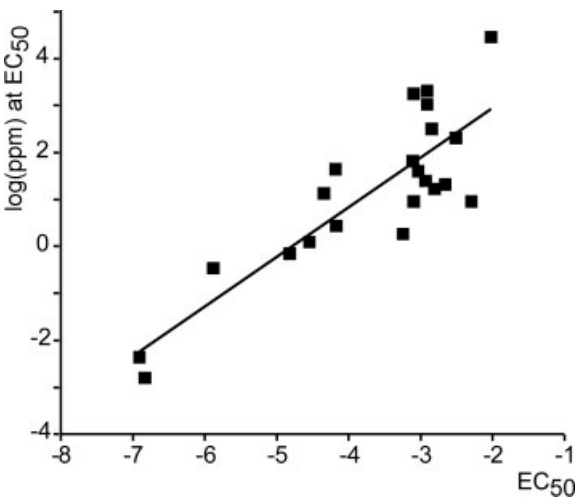

Figure 5 Plot of EC_{50} in log vol/vol concentration (X-axis) against EC_{50} in airborne log ppm (Y-axis). The two values correlate strongly (see text), with some scatter for the weaker substances (i.e., those with higher EC_{50} values).

tional hydroxyl group also led to a decreased affinity, as shown by a higher EC_{50} value [Fig. 7(D)].

We measured responses of comparable amplitudes by adjusting the concentrations (mean response ± SEM, $6 \leq n \leq 10$: *ethyl hexanaote* 10^{-5} response = 0.9 ± 0.1; *ethyl 3-hydroxy hexanoate* 10^{-3} response = 0.9 ± 0.1; *methyl hexanoate* 10^{-5} response = 1.0 ± 0.1; *methyl 3-hydroxy hexanoate* 10^{-3} = 1.0 ± 0.1; *ethyl butanoate* 10^{-4} response = 1.1 ± 0.1; *ethyl 3-(S)-(+)-hydroxy hexanoate* 10^{-2} = 1.1 ± 0.1; One-way ANOVA $F = 1.334$, $p = 0.268$). In all cases the response to the odor with the additional hydroxyl group at the 3rd carbon atom of the carboxylic acid moiety had a significantly longer rise time than the straight chain ester (*ethyl hexanoate*: rise time = 1.04 s ± 0.07 vs. *ethyl 3-hydroxy hexanoate*: rise time = 1.92 s ± 0.19, $p = 0.002$; *methyl 3-hydroxy hexanoate* = 0.95 s ± 0.11 vs. *methyl 3-hydroxy-hexanoate* rise time = 1.55 s ± 0.11, $p = 0.008$; *ethyl butanoate* rise time = 0.67 s ± 0.05 vs. *ethyl 3-(S)-(+)-hydroxy-hexanoate* rise time = 1.46 s ± 0.09, $p \leq 0.001$).

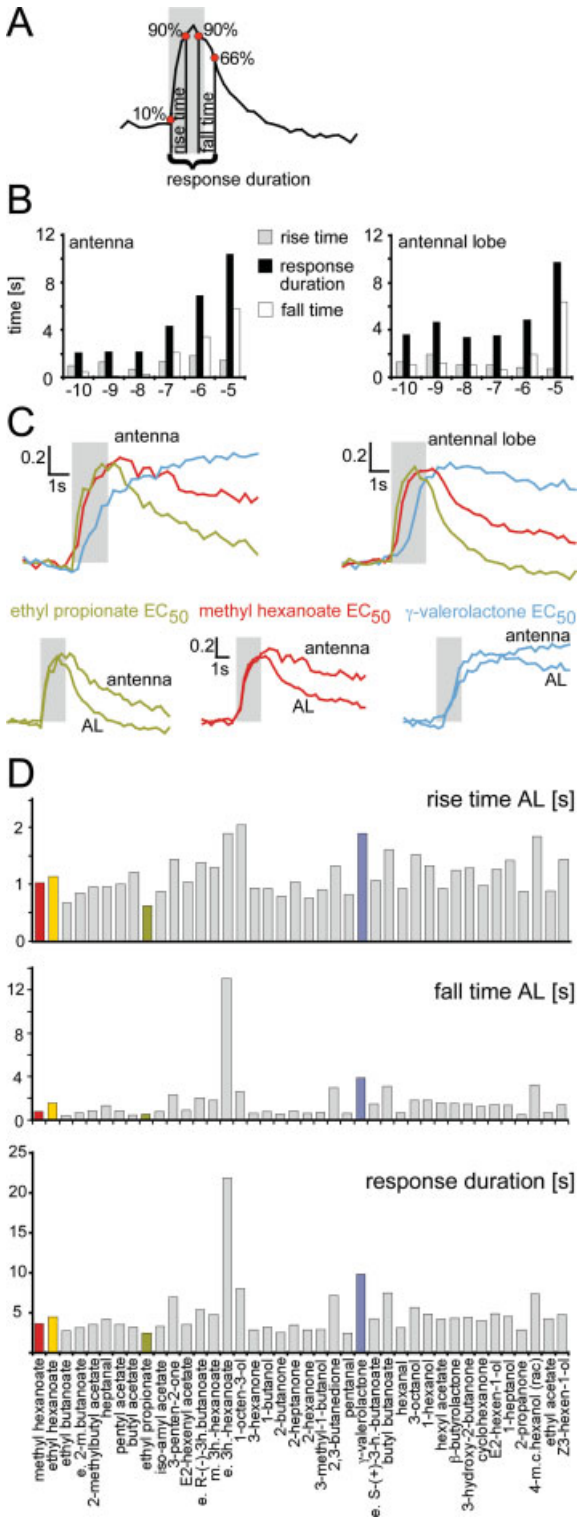

Both Best Odors and the Spectrum are Ecologically Relevant

Which are the natural odors that elicit responses in Or22a? In other words, how much of the measured response spectrum is ecologically relevant? Two scenarios compete: either the best stimuli (*ethyl hexanoate* and *methyl hexanoate*) are the only relevant odors, and the remainder of the spectrum is a laboratory finding that is irrelevant for *Drosophila* in a natural environment (the ''key substances'' hypothesis, in which Or22a effectively becomes a labeled line for *ethyl hexanoate* and *methyl hexanoate*), or the entire

Figure 6 Time course of $[Ca^{2+}]$ responses is odor and concentration dependent. **A:** Definition of response parameters of calcium responses upon presentation of an activating odor. Time points were located at 10% and 90% of maximal response on the rising shank, and at 90% and 66% on the falling shank. B: Rise time, response duration, and fall time both for antennal (*left*) and AL (*right*) measurements to increasing concentrations of *methyl hexanoate*. Response duration increases with increasing concentration. X-axis: log concentration. Panel C, *Upper:* Interpolated responses at EC_{50} to *ethyl propionate* (green), *methyl hexanoate* (red) and *γ-valerolactone* (blue) for the antenna (*left*) and the AL (*right*). Y-axis: normalized response strength. Gray rectangle: odor presentation. *Lower:* Direct comparison of the same time courses between AL and antenna. Note the slower and longer-lasting responses on the antenna. D: Time-course parameters for all activating odors. Color code as in panel C and Figure 2(B). Odors are sorted by increasing EC_{50} from left to right. From *upper* to *lower*: rise time, fall time, response duration. Y-axis: seconds. Note that there is no systematic relationship between EC_{50}-value and any of the parameters. [Color figure can be viewed in the online issue, which is available at www.interscience.wiley.com.]

spectrum is relevant, and odor identity is only extracted using information across several glomeruli (the ''combinatorial'' hypothesis). To choose between these hypotheses knowing the response spectrum alone is not sufficient, but it is necessary to compare the composition of odors that occur in the natural environment of *Drosophila* with the response spectrum of Or22a.

As a first step, we tested whether Or22a responds to banana mush, and found strong responses (data not shown), suggesting that Or22a might be involved in coding food odors. We then looked at chemical analyses of fruit extracts in the literature (Table 3). Of the substances that were identified in each fruit, many also appeared in the response spectrum of Or22a, including mango (*Mangifera indica*, 26 of 375 identified substances were among the 39 best stimuli of our screen) (Pino et al., 2005), cantaloupe melon (*Cucumis melo* var. cantalupensis, 10 of 28 substances) (Aubert and Bourger, 2004), pink guava (*Psidium guajava*, 4 of 51 substances) (Jordan et al., 2003), strawberry (*Fragaria ananassa*, 14 of 23 substances) (Loughrin and Kasperbauer, 2002), yellow passion fruit (*Passiflora edulis*, 8 of 34 substances) (Jordan et al., 2002), musk melon (*Cucumbis melo*, 10 of 38 substances) (Jordan et al., 2001a) and banana (*Musa sapientum*, 9 of 26 substances) (Jordan et al., 2001b). Based on the reported concentrations and the measured dose–response curves, we estimated which of the components occurred at sufficient concentration to elicit a half-maximal response, and found several substances in this category (Table 3). Several fruit contained *ethyl hexanoate* and/or *methyl hexanoate* at sufficient concentration. Indeed, these substances were first identified as stimuli for Or22a by screening natural odors, including passion fruit and pineapples (Stensmyr et al., 2003). Because of the high sensitivity of Or22a for these substances, minute amounts in the fruit extract are sufficient to reach significant response levels. However, other substances were present in much larger concentration, which approached or even surpassed EC_{50} even though these substances have a lower EC_{50}. For example, of the substances reported in banana extract only *isoamyl acetate* occurred at a concentration higher than EC_{50}, and *ethyl butanoate* and *hexanal* occurred at concentrations that would elicit responses, but not reach EC_{50}. In electrophysiological recordings from neurons that are likely to be ab3A neurons using banana extracts separated with a gas chromatograph, among the components that elicited responses were also *isoamyl acetate* and *ethyl butanoate* (Stensmyr et al., 2003). We conclude that many odors in the response spectrum are ecologically relevant, and that a "key substance" concept does not apply to Or22a. It should be noted, however, that this result is based on two separate datasets combined with mathematical calculations. Natural odors consist of mixtures of many substances, but mixtures were not tested in this study. Therefore, the role that mixture interaction might

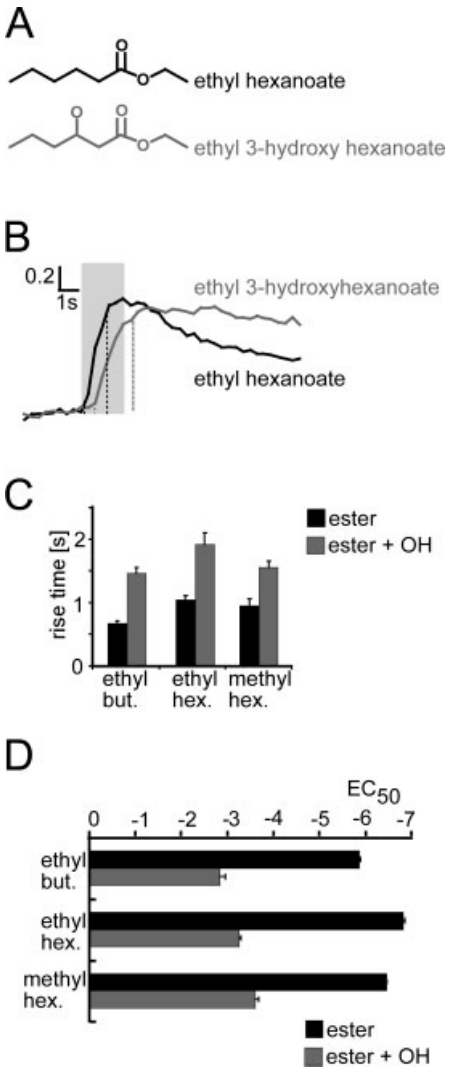

Figure 7 Relationship between chemistry of an odor and its response time course. A: Chemical structures of the ester ''pair'' *ethyl hexanoate* and *ethyl 3-hydroxy hexanoate,* which differ by the presence or absence of a hydroxyl group at the third carbon atom of the carboxylic acid moiety. B: Responses to *ethyl hexanoate* 10^{-6} (black, $n = 8$ animals) and to *ethyl 3-hydroxy hexanoate* 10^{-3} (gray, $n = 9$ other animals). Dashed lines are located at 10% and 90% of response maximum. Gray rectangle: odor presentation. Note that the two responses have very different time course but comparable maximum. C: In all three ester pairs tested the additional hydroxyl group led to an increase in the rise time of the response. D: EC_{50} values for esters with and without additional hydroxyl group. Those with the hydroxyl group were weaker stimuli (higher EC_{50}) than the respective esters without it.

Table 3 Natural sources of odors from the Or22a response spectrum

Odors Activating Or22a	Amount at EC50 [mg/kg]	Mango[a]	Melon[a]	Guava[a]	Strawberry[a]	ppm at EC50	Passion fruit[b]	Musk Melon[b]	Banana[b]
Methyl hexanoate	0.13	*0.15*			*0.67*	0.0042			
Ethyl hexanoate	0.15	*0.24*	*0.31*	*1.25*	*0.79*	0.0016	*5.08*	*0.05*	
Ethyl butanoate	1.40	*4.89*	*2.22*	1.13	0.57	0.3323	*3.86*	*0.44*	0.15
Ethyl 2-methyl butanoate	5.83	0.03	1.56		0.03	NA			
2-Methyl butyl acetate	13.75		3.40		0.05	NA			
Heptanal	15.10	0.03				0.6842			
Pentyl acetate	30.57		0.09			1.1985			
Butyl acetate	48.78	0.51	2.01		0.07	12.8830		0.38	1.32
Ethyl propionate	70.99	0.13				42.0086		0.45	
Iso-amyl acetate	72.82					2.6052			*4.85*
3-Penten-2-one	323.79	0.18				NA			
E2-hexenyl acetate	452.93				0.19	NA			
Ethyl-(*R*)-3 hydroxy butanoate	562.44	2.67				NA	6.62		
1-Octen-3-ol	580.54	0.04				1.8056			
Ethyl 3-hydroxy hexanoate	621.32	0.06				NA	2.63		
1-Butanol	766.02	4.26				64.6270		0.42	1.06
2-Heptanone	806.44	0.03				8.6482			
Hexanal	1465.28	0.22			0.06	313.7591		0.25	21.47
Butyl butanoate	1478.34	0.19			0.04	NA			0.83
Ethyl S 3 hydroxy butanoate	1737.55	2.67				NA	6.62		
1-Hexanol	2184.64	0.25	0.28		0.03	20.5361	1.56	1.09	1.17
Hexyl acetate	2554.32		2.51		0.21	NA	0.98	0.62	0.57
3-Hydroxy 2-butanone	3805.09	1.32	10.59	22.63		196.6834	27.87		
Cyclohexanone	4447.40	0.05				NA			
1-Heptanol	5042.29	0.01				8.52934			
Ethyl aceate	10398.30	4.9				28214.8984			
Z3-hexen-1-ol	10943.39	1.02	0.50	6.79	0.50	NA		2.00	

List of odors activating Or22a that were identified in various fruit. Odors are sorted by increasing amount of odor at EC_{50}. Amount at EC_{50} indicates mg odor substance per kg mineral oil. ppm at EC_{50} values were estimated as described in Methods. Names in italics indicate odors that were found in amounts sufficient to elicit at least a half-maximal response.

[a] Odors quantified as mg per kilogram fruit.

[b] Odors quantified as ppm. See results for source reference.

play for ecologically relevant stimuli remains to be assessed.

DISCUSSION

"Nihil est in intellectu quod non fuerit prius in sensu" (nothing reaches the intellect before making its appearance in the senses) is a Latin saying attributed to many empiricist philosophers. For the olfactory system, sensory input consists of all molecular receptive ranges (MRRs) of olfactory sensory neurons (OSNs). The MRR of an OSN is mostly determined not only by the OR protein expressed in it (Hallem et al., 2004), but also by odor binding proteins (Pophof, 2004; Xu et al., 2005), OSNs housed within the same sensillum (Dobritsa et al., 2003), co-receptors (Dobritsa et al., 2003; Larsson et al., 2004; Neuhaus et al., 2005; Benton et al., 2006), and G-proteins (Shirokova et al., 2005). To understand the sensory information that reaches the brain, it is therefore important to measure MRRs of OSNs *in situ* in the living animal. Here, we performed a medium-throughput screening of odor responses in genetically identified and intact OSNs in the model animal *Drosophila melanogaster,* keeping all auxiliary mechanisms and cells in place. To validate this new technique, we started with a receptor for which substantial electrophysiological data was already available (de Bruyne et al., 2001; Dobritsa et al., 2003; Stensmyr et al., 2003; Hallem et al., 2004; Wilson et al., 2004). We compared odor-evoked $[Ca^{2+}]$-signals with electrophysiologically recorded spike frequencies, and found a linear relationship between the two

over a wide portion of the dynamic range [Fig. 2(D)]. The MRR presented in this study is the first extensive analysis of more than 100 odor affinities with complete dose–response curves for an OSN both at the sensory transduction and at the synaptic transmission site. Given that the adult fly has approx. 43 expressed ORs, this study lays the foundation for a complete description of the sensory input in Drosophila.

Comparison with Other Studies

Odor responses in Or22a have been recorded in several studies (de Bruyne et al., 2001; Dobritsa et al., 2003; Stensmyr et al., 2003; Hallem et al., 2004; Wilson et al., 2004). In the most extensive of these studies, response spectra to 110 odors were reported for 21 Drosophila ORs, including Or22a, by genetically introducing the respective receptors into an empty cell, and then screening the responses electrophysiologically (Hallem and Carlson, 2006). That spectrum adds 28 active substances, and 29 non-active substances to the panel presented here, with a total of 167 substances. However, in that work odors were tested only at high concentration, and therefore the dynamic range of the responses is not available, with exception of a small subset of odors. However, odor receptors have evolved to code both odor identity and odor concentration, and odor plumes generally contain odors at low concentration. Our semi-automated technique allows to measure entire dose–response curves, and therefore to characterize receptors in a great detail. For example, it is only by knowing the entire dose–response curve that we can show that secondary ligands are also important in an ecological context. We share the goal to completely understand the olfactory input for this model animal. A detailed comparison between the spectrum found by Hallem and Carlson and in this study is given in the supplementary Figure 2. The two data sets correspond well, but the scatter increases at the higher spike-value end. This discrepancy arises from the saturation of the responses when tested only at high concentration (as done in Hallem), again showing that measuring entire dose–response curves gives better information. Hallem and Carlson measured all receptors by expressing the receptor in the ab3A cell. In ab3A, Or22a is the native receptor. We anticipate that with other receptors the mismatch between the two techniques will increase, because different cells do not only differ in the receptors they express, but also in other aspects, such as OBPs and maybe intracellular messenger cascades. By expressing the calcium sensor in the receptors' native cells, our approach avoids a mismatch between receptor and cellular environment.

Comparison between Antennal and AL Measurements

We used intracellular [Ca^{2+}] changes as monitor for cellular activity by expressing the genetically encoded calcium sensor *cameleon2.1* in those OSNs that express *Or22a*. However, each OSN has two mechanistically very different and spatially segregated calcium-compartments. First, at the sensory dendrites, calcium is involved in signal transduction, as shown in vertebrates (Matthews and Reisert, 2003) and insects (Stengl, 1994). Second, at the axonal terminals, calcium is involved in transmitter release. Calcium in the dendrites is correlated with the elicited receptor potential, and might be a combination of extracellular calcium entering through second-messenger-gated Ca-channels, voltage gated Ca-channels (VOCs) and calcium from intracellular stores. Here, calcium plays a dual role in sensory transduction and adaptation (Matthews and Reisert, 2003). In our antenna measurements, we also measured fluorescence from cell bodies. In invertebrate sensory neurons, cell bodies respond to stimulation with delayed intracellular calcium increase (Höger et al., 2005). At the synaptic terminals, calcium entry occurs through VOCs, and within a certain range is proportional to AP firing frequency [Fig. 2(D)]. However, presynaptic inhibition might modify this relationship, for example when opened chloride channels shunt the incoming depolarization, and thus prevent calcium influx even in the presence of APs. Presynaptic inhibition of OSNs is known for several vertebrates and invertebrates (Wachowiak and Cohen, 1998; Wachowiak and Cohen, 1999; Aroniadou-Anderjaska et al., 2000; Ennis et al., 2001; Wachowiak et al., 2005), and is likely to occur in *Drosophila* too.

To quantify the difference between those compartments, we established the MRR of Or22a both on the antenna and in the AL. There was no significant difference in the response spectrum (see Fig. 3), suggesting that at this level presynaptic inhibition, if present, does not modify the MRR. We cannot exclude, however, that presynaptic inhibition onto OSN terminals might occur and have more subtle effects. Indeed, responses in the antenna and the AL were not identical. Differences in time course could be partially caused by inhibitory mechanisms that are slow, possibly mediated by metabotropic receptors. Presynaptic $GABA_B$ receptors on vertebrate olfactory OSN terminals modulate presynaptic calcium influx (Aroniadou-Anderjaska et al., 2000; Wachowiak et al., 2005). The entire response-spectrum was shifted on the antenna by 0.5 log units. This could be due to a difference in resting [Ca^{2+}] level. Because

any calcium sensor only measures a limited concentration range, which in the case of *Cameleon2.1* is approx 30 n*M* to 100 μM (Miyawaki et al., 1999), a shift in baseline level [Ca^{2+}] changes the set-point of the indicator. This is evidenced by the responses to *4-methoxybenzene* [Fig. 2(C)] and *benzaldehyde*. On the antenna these odors evoked a decrease in measured [Ca^{2+}] while they did not evoke any change in the AL. However, after stimulation with an odor that evoked a long-lasting response both odors also lead to a decrease in measured [Ca^{2+}] within the AL, most likely due to an increased [Ca^{2+}] level. This finding has further implications: we show that a strong stimulus leads to a modified response to another stimulus that occurs later in time, and this modification is not adaptation. We did not analyze this aspect further, but we anticipate that it might have important implications for an animal flying in a natural environment, and encountering different odor plumes in sequence. Specifically, for example, a plume of *benzaldehyde* will elicit an activity decrease in glomerulus DM2 after a plume of *ethyl hexanoate* but no change before such a plume. In other words, the glomerular response pattern to *benzaldehyde* is context dependent. More research is needed to address this question.

Our finding that some stimuli lead to a decrease in [Ca^{2+}] confirms electrophysiological findings of inhibitory responses to some odor/receptor combinations (de Bruyne et al., 1999, 2001). Possibly, Or22a is a constitutively active OR, and inactivating odors act as inverse agonists, as increasingly reported for many GPCRs (Costa and Cotecchia, 2005). It should be noted that our experimental design is suitable to identify inverse agonists in cells with constitutively active receptors, but not to find competitive antagonists. Experiments with odor mixtures will be necessary to find competitive antagonists, as shown for *citral* in the rat I7 receptor (Araneda et al., 2000).

Specialist Versus Generalist

OSNs may be specialists that respond to a few key substances, or generalists that respond to a large number of odors (Hildebrand and Shepherd, 1997). 38% of the 104 substances tested initially gave at least half-maximal responses at 10^{-2} dilution. This might suggest a generalist response characteristic. However, the sensitivity to different substances varied enormously. For example, *ethyl hexanoate* and *methyl hexanoate* reached half-maximal responses already at a dilution greater than 10^{-6} (Table 1). Because these substances are important components in many fruits, Or22a might be a specialist for these two substances. However, whether Or22a should be considered a specialist or rather a generalist solely depends on the naturally occurring concentrations of the respective substances in odor sources that flies encounter. We therefore compared the sensitivities found in our screen with the concentration of these substances in natural odor sources, and found that several of the 10 best odors occur at sufficient concentration in nature to elicit responses in Or22a, including *methyl hexanoate*, *ethyl butanoate* and *isoamyl acetate* (Table 3). Therefore, although Or22a is most sensitive to *ethyl hexanoate*, this is not the only ecologically relevant substance: it is inappropriate to call Or22a an *ethyl hexanoate*-receptor. In a behavioral study in adult *Drosophila*, removing Or22a did not create a defect for *ethyl hexanoate* perception, but rather for *1-heptanol* (A. Keller and L. Vosshall, personal communication). Clearly, the ecological and behavioral relevance of the odors within the MRR remains to be explored in detail. An extension into odor mixtures is necessary to answer this question.

Odotopes for Or22a

So far no olfactory receptor has been crystallized. Therefore, information on interaction sites between an odor and its receptor has to come either from testing many substances with one receptor (as done here for the OSN), or by genetically modifying the receptor and monitor ligand changes (Luu et al., 2004; Katada et al., 2005).

For Or22a the preferred functional group was an ester. This was not strict given that several good ligands were not esters, but aldehydes, ketones, alcohols or oxygen heteroaromates. All had an oxygen atom, which might act as hydrogen acceptor, suggesting the presence of a hydrogen donor within the binding site of Or22a, as has been proposed for a serine residue in the mouse *eugenol* receptor (Katada et al., 2005). There were clear molecular constraints on the spatial configuration of activating esters. Increasing the chain length on either side led to a quicker drop in sensitivity than shortening it (see Fig. 4). In other words, increased concentrations partially compensate for molecules that are smaller than optimal, but not for those that are larger. Possibly, smaller molecules can still interact with the receptor, but may not reside stably within the binding site and dissociate faster. As for other ORs (Araneda et al., 2000; Spehr et al., 2003), the binding pocket recognizes several characteristics of the odor molecule that are not independent from each other. As a consequence, an ''odotope'' cannot be regarded as an olfactory molecule's part (such as, say, an ''aldehyde''), but rather as a combination of properties. Predictive modeling followed by

experimental testing will further elucidate the interactions between receptor and ligand.

In this study, we have characterized the responses of OSNs that express *Or22a* to a large panel of odorants across concentrations. This has been possible by a combination of calcium imaging with genetic tools (expression of a calcium sensor in a homogeneous population of OSNs) and robotics (automated presentation of odors). The antennal preparation is done in an intact animal, and affords the opportunity to measure for long times in a single individual. We could thus draw a differentiated picture of Or22a. Despite reacting to a large number of odors very specific ligands exist. The segregation of generalist and specialist receptors appears inappropriate, because Or22a is both. A full characterization of the entire input to *Drosophila* as an important model appears now in reach.

Thanks to Beate Eisermann and Gabi Haberberger for excellent technical assistance, and to Dan Jeske (UCR statistical consulting) for statistical advise. Thanks to Ana Silbering, Silke Sachse, and Philipp Peele for comments on the manuscript, thanks to Christian Markl, Hajo Hach, Annika Waibel, Anja Nissler, and Daniel Siever for help with data analysis, and thanks to Randolf Menzel for continued support, both material and intellectual. Fly lines were kindly provided by Leslie Vosshall and André Fiala.

REFERENCES

Araneda RC, Kini AD, Firestein S. 2000. The molecular receptive range of an odorant receptor. Nat Neurosci 3:1248–1255.

Aroniadou-Anderjaska V, Zhou FM, Priest CA, Ennis M, Shipley MT. 2000. Tonic and synaptically evoked presynaptic inhibition of sensory input to the rat olfactory bulb via GABA(B) heteroreceptors. J Neurophysiol 84:1194–1203.

Aubert C, Bourger N. 2004. Investigation of volatiles in Charentais cantaloupe melons (*Cucumis melo* var cantalupensis). Characterization of aroma constituents in some cultivars. J Agric Food Chem 52:4522–4528.

Benton R, Sachse S, Michnick SW, Vosshall LB. 2006. Atypical membrane topology and heteromeric function of Drosophila odorant receptors in vivo. PLoS Biol 4:e20.

Bhalerao S, Sen A, Stocker R, Rodrigues V. 2003. Olfactory neurons expressing identified receptor genes project to subsets of glomeruli within the antennal lobe of *Drosophila melanogaster*. J Neurobiol 54:577–592.

Bozza T, Feinstein P, Zheng C, Mombaerts P. 2002. Odorant receptor expression defines functional units in the mouse olfactory system. J Neurosci 22:3033–3043.

Buck L, Axel R. 1991. A novel multigene family may encode odorant receptors: A molecular basis for odor recognition. Cell 65:175–187.

Clyne PJ, Warr CG, Freeman MR, Lessing D, Kim J, Carlson JR. 1999. A novel family of divergent seven-transmembrane proteins: Candidate odorant receptors in *Drosophila*. Neuron 22:327–338.

Cometto-Muniz JE, Cain WS, Abraham MH. 2003. Quantification of chemical vapors in chemosensory research. Chem Senses 28:467–477.

Costa T, Cotecchia S. 2005. Historical review: Negative efficacy and the constitutive activity of G-protein-coupled receptors. Trends Pharmacol Sci 26:618–624.

Couto A, Alenius M, Dickson BJ. 2005. Molecular, anatomical, and functional organization of the Drosophila olfactory system. Curr Biol 15:1535–1547.

de Bruyne M, Clyne PJ, Carlson JR. 1999. Odor coding in a model olfactory organ: The *Drosophila* maxillary palp. J Neurosci 19:4520–4532.

de Bruyne M, Foster K, Carlson JR. 2001. Odor coding in the Drosophila antenna. Neuron 30:537–552.

Dobritsa AA, van der Goesvan Naters W, Warr CG, Steinbrecht RA, Carlson JR. 2003. Integrating the molecular and cellular basis of odor coding in the *Drosophila* antenna. Neuron 37:827–841.

Ennis M, Zhou FM, Ciombor KJ, Aroniadou-Anderjaska V, Hayar A, Borrelli E, Zimmer LA, et al. 2001. Dopamine D2 receptor-mediated presynaptic inhibition of olfactory nerve terminals. J Neurophysiol 86:2986–2997.

Estes PS, Roos J, van der Bliek A, Kelly RB, Krishnan KS, Ramaswami M. 1996. Traffic of dynamin within individual Drosophila synaptic boutons relative to compartment-specific markers. J Neurosci 16:5443–5456.

Fiala A, Spall T, Diegelmann S, Eisermann B, Sachse S, Devaud JM, Buchner E, et al. 2002. Genetically expressed cameleon in *Drosophila melanogaster* is used to visualize olfactory information in projection neurons. Curr Biol 12:1877–1884.

Fishilevich E, Vosshall LB. 2005. Genetic and functional subdivision of the Drosophila antennal lobe. Curr Biol 15:1548–1553.

Gao Q, Chess A. 1999. Identification of candidate Drosophila olfactory receptors from genomic DNA sequence. Genomics 60:31–39.

Grosmaitre X, Vassalli A, Mombaerts P, Shepherd GM, Ma M. 2006. Odorant responses of olfactory sensory neurons expressing the odorant receptor MOR23: A patch clamp analysis in gene-targeted mice. Proc Natl Acad Sci USA 103:1970–1975.

Hallem EA, Carlson JR. 2006. Coding of odors by a receptor repertoire. Cell 125:143–160.

Hallem EA, Ho MG, Carlson JR. 2004. The molecular basis of odor coding in the *Drosophila* antenna. Cell 117:965–979.

Hildebrand JG, Shepherd GM. 1997. Mechanisms of olfactory discrimination: Converging evidence for common principles across phyla. Annu Rev Neurosci 20:595–631.

Höger U, Torkkeli PH, French AS. 2005. Calcium concentration changes during sensory transduction in spider mechanoreceptor neurons. Eur J Neurosci 22:3171–3178.

Jordan MJ, Goodner KL, Shaw PE. 2002. Characterization of the aromatic profile in aqueous essence and fruit juice of

yellow passion fruit (*Passiflora edulis* Sims F. Flavicarpa degner) by GC-MS and GC/O. J Agric Food Chem 50:1523–1528.

Jordan MJ, Margaria CA, Shaw PE, Goodner KL. 2003. Volatile components and aroma active compounds in aqueous essence and fresh pink guava fruit puree (*Psidium guajava* L.) by GC-MS and multidimensional GC/GC-O. J Agric Food Chem 51:1421–1426.

Jordan MJ, Shaw PE, Goodner KL. 2001a. Volatile components in aqueous essence and fresh fruit of *Cucumis melo* cv. Athena (muskmelon) by GC–MS and GC–O. J Agric Food Chem 49:5929–5933.

Jordan MJ, Tandon K, Shaw PE, Goodner KL. 2001b. Aromatic profile of aqueous banana essence and banana fruit by gas chromatography–mass spectrometry (GC–MS) and gas chromatography–olfactometry (GC–O). J Agric Food Chem 49:4813–4817.

Katada S, Hirokawa T, Oka Y, Suwa M, Touhara K. 2005. Structural basis for a broad but selective ligand spectrum of a mouse olfactory receptor: Mapping the odorant-binding site. J Neurosci 25:1806–1815.

Laissue PP, Reiter C, Hiesinger PR, Halter S, Fischbach KF, Stocker RF. 1999. Three-dimensional reconstruction of the antennal lobe in *Drosophila melanogaster*. J Comp Neurol 405:543–552.

Larsson MC, Domingos AI, Jones WD, Chiappe ME, Amrein H, Vosshall LB. 2004. Or83b encodes a broadly expressed odorant receptor essential for *Drosophila* olfaction. Neuron 43:703–714.

Lewcock JW, Reed RR. 2004. A feedback mechanism regulates monoallelic odorant receptor expression. Proc Natl Acad Sci USA 101:1069–1074.

Loughrin JH, Kasperbauer MJ. 2002. Aroma of fresh strawberries is enhanced by ripening over red versus black mulch. J Agric Food Chem 50:161–165.

Luu P, Acher F, Bertrand HO, Fan J, Ngai J. 2004. Molecular determinants of ligand selectivity in a vertebrate odorant receptor. J Neurosci 24:10128–10137.

Malnic B, Hirono J, Sato T, Buck LB. 1999. Combinatorial receptor codes for odors. Cell 96:713–723.

Matthews HR, Reisert J. 2003. Calcium, the two-faced messenger of olfactory transduction and adaptation. Curr Opin Neurobiol 13:469–475.

Meister M, Bonhoeffer T. 2001. Tuning and topography in an odor map on the rat olfactory bulb. J Neurosci 21:1351–1360.

Miyawaki A, Griesbeck O, Heim R, Tsien RY. 1999. Dynamic and quantitative Ca^{2+} measurements using improved cameleons. Proc Natl Acad Sci USA 96:2135–2140.

Mombaerts P, Wang F, Dulac C, Chao SK, Nemes A, Mendelsohn M, Edmondson J, et al. 1996. Visualizing an olfactory sensory map. Cell 87:675–686.

Mori K, Shepherd GM. 1994. Emerging principles of molecular signal processing by mitral/tufted cells in the olfactory bulb. Semin Cell Biol 5:65–74.

Motulsky H, Christopoulos A. 2004. Fitting Models to Biological Data Using Linear and Nonlinear Regression. Oxford: Oxford University Press, 351p.

Neuhaus EM, Gisselmann G, Zhang W, Dooley R, Stortkuhl K, Hatt H. 2005. Odorant receptor heterodimerization in the olfactory system of *Drosophila melanogaster*. Nat Neurosci 8:15–17.

Pino JA, Mesa J, Munoz Y, Marti MP, Marbot R. 2005. Volatile components from mango (*Mangifera indica* L.) cultivars. J Agric Food Chem 53:2213–2223.

Pophof B. 2004. Pheromone-binding proteins contribute to the activation of olfactory receptor neurons in the silkmoths antheraea polyphemus and *Bombyx mori*. Chem Senses 29:117–125.

Reiff DF, Ihring A, Guerrero G, Isacoff EY, Joesch M, Nakai J, Borst A. 2005. In vivo performance of genetically encoded indicators of neural activity in flies. J Neurosci 25: 4766–4778.

Reisert J, Matthews HR. 2001. Simultaneous recording of receptor current and intraciliary Ca^{2+} concentration in salamander olfactory receptor cells. J Physiol 535:637–645.

Ressler KJ, Sullivan SL, Buck LB. 1994. Information coding in the olfactory system: Evidence for a stereotyped and highly organized epitope map in the olfactory bulb. Cell 79:1245–1255.

Sachse S, Galizia CG. 2003. The coding of odour-intensity in the honeybee antennal lobe: Local computation optimizes odour representation. Eur J Neurosci 18:2119–2132.

Serizawa S, Miyamichi K, Nakatani H, Suzuki M, Saito M, Yoshihara Y, Sakano H. 2003. Negative feedback regulation ensures the one receptor-one olfactory neuron rule in mouse. Science 302:2088–2094.

Shirokova E, Schmiedeberg K, Bedner P, Niessen H, Willecke K, Raguse JD, Meyerhof W, et al. 2005. Identification of specific ligands for orphan olfactory receptors. G protein-dependent agonism and antagonism of odorants. J Biol Chem 280:11807–11815.

Spehr M, Gisselmann G, Poplawski A, Riffell JA, Wetzel CH, Zimmer RK, Hatt H. 2003. Identification of a testicular odorant receptor mediating human sperm chemotaxis. Science 299:2054–2058.

Stengl M. 1994. Inositol-trisphosphate-dependent calcium currents precede cation currents in insect olfactory receptor neurons in vitro. J Comp Physiol [A] 174:187–194.

Stensmyr MC, Giordano E, Balloi A, Angioy AM, Hansson BS. 2003. Novel natural ligands for Drosophila olfactory receptor neurones. J Exp Biol 206:715–724.

Stocker RF. 1994. The organization of the chemosensory system in *Drosophila melanogaster*: A review. Cell Tissue Res 275:3–26.

Stocker RF. 2001. Drosophila as a focus in olfactory research: Mapping of olfactory sensilla by fine structure, odor specificity, odorant receptor expression, and central connectivity. Microsc Res Tech 55:284–296.

Stocker RF, Lienhard MC, Borst A, Fischbach KF. 1990. Neuronal architecture of the antennal lobe in *Drosophila melanogaster*. Cell Tissue Res 262:9–34.

Takeuchi H, Kurahashi T. 2005. Mechanism of signal amplification in the olfactory sensory cilia. J Neurosci 25:11084–11091.

Vassar R, Chao SK, Sitcheran R, Nu~nez JM, Vosshall LB, Axel R. 1994. Topographic organization of sensory projections to the olfactory bulb. Cell 79:981–991.

Vosshall LB, Amrein H, Morozov PS, Rzhetsky A, Axel R. 1999. A spatial map of olfactory receptor expression in the *Drosophila* antenna. Cell 96:725–736.

Vosshall LB, Wong AM, Axel R. 2000. An olfactory sensory map in the fly brain. Cell 102:147–159.

Wachowiak M, Cohen LB. 1998. Presynaptic afferent inhibition of lobster olfactory receptor cells: Reduced action-potential propagation into axon terminals. J Neurophysiol 80:1011–1015.

Wachowiak M, Cohen LB. 1999. Presynaptic inhibition of primary olfactory afferents mediated by different mechanisms in lobster and turtle. J Neurosci 19:8808–8817.

Wachowiak M, Cohen LB. 2001. Representation of odorants by receptor neuron input to the mouse olfactory bulb. Neuron 32:723–735.

Wachowiak M, McGann JP, Heyward PM, Shao Z, Puche AC, Shipley MT. 2005. Inhibition of olfactory receptor neuron input to olfactory bulb glomeruli mediated by suppression of presynaptic calcium influx. J Neurophysiol 94:2700–2712.

Wilson RI, Turner GC, Laurent G. 2004. Transformation of olfactory representations in the Drosophila antennal lobe. Science 303:366–370.

Xu P, Atkinson R, Jones DN, Smith DP. 2005. Drosophila OBP LUSH is required for activity of pheromone-sensitive neurons. Neuron 45:193–200.